

## A POSTERIORI ERROR ESTIMATE FOR STABILIZED FINITE ELEMENT METHODS FOR THE STOKES EQUATIONS

JUNPING WANG, YANQIU WANG, AND XIU YE

**Abstract.** Computation with adaptive grid refinement has proved to be a useful and efficient tool in scientific computing over the last several decades. The key behind this technique is the design of a good a posteriori error estimator that provides a guidance on how and where grids should be refined. In this paper, the authors propose and analyze a posteriori error estimator for a stabilized finite element method in computational fluid dynamics. The main contributions of the paper are: (1) an efficient a posteriori error estimator is designed and analyzed for a general stabilized finite element method, (2) a rigorous mathematical analysis is established for a theoretical justification of its efficiency and generality to other applications, and (3) some computational results with a comparison with other methods are presented for a computational justification of the proposed a posteriori error estimator.

**Key Words.** A posteriori error estimate, finite element methods, CFD, adaptive grid refinement

### 1. Introduction

Computation with adaptive grid refinement has proved to be a useful and efficient tool in scientific computing over the last several decades. The key behind this technique is the design of a good posteriori error estimator that provides a guidance on how and where grids should be refined. The goal of this manuscript is to propose and analyze a posteriori error estimator for a stabilized finite element method in computational fluid dynamics.

As was well-known in the analysis and employment of finite element methods in solving the Navier-Stokes equations, the inf-sup condition [3] has played an important role because it ensures a stability and accuracy of the underlying numerical schemes. A pair of finite element spaces that are used to approximate the velocity and the pressure unknowns are said to be stable if they satisfy the inf-sup condition. Intuitively speaking, the inf-sup condition is a measure that enforces a certain correlation between two finite element spaces so that they both have the required properties when employed for approximating the Navier-Stokes equations. It is well known that the two simplest elements  $P_1/P_0$  (i.e., linear/constant) on triangle and  $Q_1/P_0$  (i.e., bilinear/constant) on quadrilateral do not satisfy the inf-sup condition. Furthermore, they are known to be not stable, and therefore can not be trusted when employed in practical computation. In contrast, most known stable elements

---

Received by the editors February 10, 2009 and, in revised form, August 16, 2009.

1991 *Mathematics Subject Classification.* Primary, 65N15, 65N30, 76D07; Secondary, 35B45, 35J50 .

The research of Xiu Ye was supported in part by National Science Foundation Grant DMS-0813571.

do not seem to be natural because their construction involves non-standard functions or polynomials which are not commonly used/implemented in popular engineering code packages. To eliminate the constraint of the inf-sup condition so that natural finite element spaces can be used, several stabilized finite element methods have been developed for the Stokes equations in the last two decades [12, 4, 13, 8]. These methods are gaining more and more popularity in computational fluid dynamics, and this paper is focused on a further study of them.

For simplicity, the study shall be conducted for the incompressible Stokes equation for which the stabilized method as proposed in [8] is employed. The main contributions of this paper are: (1) an efficient a posteriori error estimator is designed and analyzed for the said stabilized finite element method, (2) a rigorous mathematical analysis is established for a theoretical justification of its efficiency and generality to other model equations, and (3) some computational results with a comparison with other methods are presented for a computational justification of the proposed a priori error estimator.

It should be pointed out that a posteriori error estimators for the  $P_1/P_0$  stabilized finite element methods have been studied by Kay and Silvester [14]. The error estimators as proposed in [14] are of residual type which is strongly related to the a priori error estimator to be presented in this paper. However, the result of this paper applies to finite elements of arbitrary order, and the grid refinement strategies are different from that of [14].

The research of one of the authors was heavily influenced by his connection with Dr. Richard Ewing, particularly in the area of fluid dynamics and grid local refinement techniques for finite element methods. In fact, the first time when this author learnt “grid local refinement” was through a lecture presented by Dr. Ewing in 1987 at the Institute of Mathematics and Its Applications, University of Minnesota. Dr. Ewing had been a long time advocator for promoting the use and research of grid local refinements in scientific computing. This paper was written in the memory of Dr. Ewing for his scientific stimulation and vision in the research of computational mathematics.

The paper is organized as follows. In Section 2, we review some notations and outline a stabilized finite element formulation for the Stokes equations. In Section 3, a posteriori error estimator is given and a theoretical justification for its reliability and efficiency is established. Finally in Section 4, we present some numerical experiments for three test problems with two different refinement strategies.

## 2. Preliminaries and the stabilized finite element method

For simplicity, we consider the homogeneous Dirichlet boundary value problem for the Stokes equations. This model problem seeks unknown functions  $\mathbf{u} \in H^1(\Omega)^d$  and  $p \in L^2(\Omega)$  satisfying

$$\begin{aligned} (1) \quad & -\nu \Delta \mathbf{u} + \nabla p = \mathbf{f} \quad \text{in } \Omega, \\ (2) \quad & \nabla \cdot \mathbf{u} = 0 \quad \text{in } \Omega, \\ (3) \quad & \mathbf{u} = 0 \quad \text{on } \partial\Omega, \end{aligned}$$

where  $\Omega$  is an open bounded domain in the Euclidean space  $\mathbf{R}^d$  ( $d = 2, 3$ ) with a Lipschitz continuous boundary  $\partial\Omega$ ;  $\mathbf{f}$  is a given function in  $H^{-1}(\Omega)^d$ ;  $\Delta$ ,  $\nabla$ , and  $\nabla \cdot$  denote the Laplacian, gradient, and divergence operators respectively;  $\nu > 0$  is a given constant representing the viscosity of the fluid. The given function/distribution  $\mathbf{f} = \mathbf{f}(x)$  is the unit external volumetric force acting on the fluid at  $x \in \Omega$ . Without

loss of generality, we assume that  $\nu = 1$ ,  $d = 2$ , and  $\Omega$  is polygonal in the rest of the paper.

The above description of the Stokes problem has assumed the standard notation for the Sobolev spaces  $H^s(\Omega)$  which is the collection of distributions whose weak derivatives of order up to  $s$  are square integrable functions over the domain  $\Omega$ . Denote by  $(\cdot, \cdot)_s$  the inner product associated with  $H^s(\Omega)$ , with a norm notation  $\|\cdot\|_s$ , and semi-norm notation  $|\cdot|_s$  for non-negative integers  $s \geq 0$ . The Sobolev space  $H^0(\Omega)$  coincides with the space of square integrable functions  $L^2(\Omega)$ , in which case the norm and inner product are denoted by  $\|\cdot\|$  and  $(\cdot, \cdot)$ , respectively. In addition, denote by  $L_0^2(\Omega)$  the subspace of  $L^2(\Omega)$  consisting of all the functions in  $L^2(\Omega)$  with vanishing mean value, and  $H_0^1(\Omega)$  stands for the closed subspace of  $H^1(\Omega)$  with vanishing boundary values on  $\Omega$ . In general,  $\|\phi\|_D$  denotes the  $L^2$  norm of  $\phi \in L^2(D)$  for any domain  $D$ .

Let  $V_h \subset [H_0^1(\Omega)]^2$  and  $W_h \subset L_0^2(\Omega)$  be two finite element spaces consisting of piecewise polynomials for the velocity and pressure unknowns, respectively, associated with a prescribed finite element partition  $\mathcal{T}_h$ . Let  $\mathcal{E}_h$  be the set of all edges in  $\mathcal{T}_h$  and  $\mathcal{E}_h^0 := \mathcal{E}_h \setminus \partial\Omega$ . Let  $e \in \mathcal{E}_h^0$  be an interior edge shared by two elements  $T_1$  and  $T_2$  in  $\mathcal{T}_h$ . We denote by  $[q]$  the jump of  $q$  on  $e$ :

$$[q] = q|_{T_1} - q|_{T_2},$$

where  $q|_{T_i}$  is the trace of  $q$  on  $e$  as seen from the element  $T_i$  for  $i = 1, 2$ . It should be pointed out that interchanging the role of  $T_1$  and  $T_2$  in the jump definition will have no effect on the finite element scheme to be described shortly in this section.

Let  $\beta$  and  $\gamma$  be two parameters to be determined later and  $\tau = \pm 1$ . Define a bilinear form as follows:

$$\begin{aligned} \Phi(\mathbf{w}, r; \mathbf{v}, q) &= (\nabla \mathbf{w}, \nabla \mathbf{v}) - (\nabla \cdot \mathbf{v}, r) - (\nabla \cdot \mathbf{w}, q) \\ &\quad - \gamma \sum_{T \in \mathcal{T}_h} h_T^2 (\nabla r - \Delta \mathbf{w}, \nabla q - \tau \Delta \mathbf{v})_T - \beta \sum_{e \in \Gamma_0} h_e ([r], [q])_e, \end{aligned}$$

where  $(p, q)_e = \int_e pq \, ds$  is the  $L^2$ -inner product in  $L^2(e)$ . The corresponding stabilized finite element formulation for the Stokes equations seeks  $(\mathbf{u}_h; p_h) \in V_h \times W_h$  such that for all  $(\mathbf{v}; q) \in V_h \times W_h$

$$(4) \quad \Phi(\mathbf{u}_h, p_h; \mathbf{v}, q) = (\mathbf{f}, \mathbf{v}) - \gamma \sum_{T \in \mathcal{T}_h} h_T^2 (\mathbf{f}, \nabla q - \tau \Delta \mathbf{v})_T.$$

It is not hard to see that the exact solution  $(\mathbf{u}; p)$  of the Stokes equations also satisfies (4) for any values of  $\beta$  and  $\gamma$ . Thus, the following error equation is easy to verify:

$$(5) \quad \Phi(\mathbf{u} - \mathbf{u}_h, p - p_h; \mathbf{v}, q) = 0, \quad \forall \mathbf{v} \in V_h, \forall q \in W_h.$$

If  $q = 0$ , the above error equation becomes

$$(6) \quad (\nabla \mathbf{e}, \nabla \mathbf{v}) - (\nabla \cdot \mathbf{v}, \epsilon) + \gamma \sum_{T \in \mathcal{T}_h} h_T^2 (\nabla \epsilon - \Delta \mathbf{e}, \tau \Delta \mathbf{v})_T = 0, \quad \forall \mathbf{v} \in V_h$$

where  $\mathbf{e} = \mathbf{u} - \mathbf{u}_h$  and  $\epsilon = p - p_h$ .

Observe that the bilinear form  $\Phi(\cdot; \cdot)$  is symmetric for  $\tau = 1$ , and is nonsymmetric for  $\tau = -1$ . It was proved that the symmetric formulation is conditionally stable with respect to the positive parameter values of  $\gamma$  and  $\beta$  where  $\beta$  could assume arbitrary values. The nonsymmetric scheme is absolutely stable with respect to positive parameter values of  $\gamma$  and  $\beta$ . Details can be found in [8, 15].

Define a norm in  $V_h \times W_h$  by

$$|(\mathbf{v}; q)|^2 = \|\nabla \mathbf{v}\|^2 + \sum_{T \in \mathcal{T}_h} h_T^2 \|\nabla q\|_T^2 + \sum_{e \in \mathcal{E}_h^0} h_e ([q], [q])_e.$$

We have the following a priori error estimation [15]:

**Theorem 1.** *Let  $(\mathbf{u}_h; p_h) \in V_h \times W_h$  and  $(\mathbf{u}; p) \in (H^{k+1}(\Omega) \cap H_0^1(\Omega))^2 \times H^k(\Omega) \cap L_0^2(\Omega)$  be the solutions of (4) and (1)-(3) respectively. Then there exists a constant  $C$  independent of  $h$  such that*

$$(7) \quad |(\mathbf{u} - \mathbf{u}_h; p - p_h)| \leq Ch^k (\|\mathbf{u}\|_{k+1} + \|p\|_k).$$

### 3. A posteriori error estimates

Let  $e$  be an interior edge shared by two elements  $T_1$  and  $T_2$  in  $\mathcal{T}_h$ , and let  $\mathbf{n}_1$  and  $\mathbf{n}_2$  be unit normal vectors on  $e$  pointing outward to  $T_1$  and  $T_2$ , respectively. We define

$$[[\nabla \mathbf{u}_h - p_h I]]_e = (\nabla \mathbf{u}_h - p_h I)|_{\partial T_1} \cdot \mathbf{n}_1 + (\nabla \mathbf{u}_h - p_h I)|_{\partial T_2} \cdot \mathbf{n}_2.$$

We are now in a position to describe a posteriori error estimator for the stabilized finite element formulation of the Stokes equations. Let  $I$  be the  $2 \times 2$  identity matrix and let

$$\mathbf{J}(\nabla \mathbf{u}_h - p_h I) = \begin{cases} [[\nabla \mathbf{u}_h - p_h I]]_e & \text{if } e \in \mathcal{E}_h^0 \\ 0 & \text{otherwise.} \end{cases}$$

We define a global error estimator by

$$\eta^2 = \sum_{T \in \mathcal{T}_h} \eta_T^2,$$

with

$$\eta_T^2 = h_T^2 \|\mathbf{f} + \Delta \mathbf{u}_h - \nabla p_h\|_T^2 + \|\nabla \cdot \mathbf{u}_h\|_T^2 + \frac{1}{2} \sum_{e \in \partial T} \int_e h_e \mathbf{J}(\nabla \mathbf{u}_h - p_h I)^2 ds.$$

**3.1. Reliability of the estimator.** It is easy to see that there exists a constant  $C$  such that for any function  $g \in H^1(K)$

$$(8) \quad \|g\|_e^2 \leq C (h_K^{-1} \|g\|_K^2 + h_K \|\nabla g\|_K^2).$$

**Lemma 1.** *Let  $(\mathbf{u}; p)$  and  $(\mathbf{u}_h; p_h)$  be the solutions of (1)-(2) and (4). Then we have*

$$(9) \quad \|p - p_h\|^2 \leq C(\eta^2 + \|\nabla \mathbf{e}\|^2).$$

*Proof.* Let  $\mathbf{v} \in H_0^1(\Omega)^2$  and  $\mathbf{v}_I \in V_h$  be the Clement interpolation of  $\mathbf{v}$  as described in [6] by using local averaging techniques around each interior nodal point. Using

integration by parts, equations (6), (8) and the inverse inequality, we obtain

$$\begin{aligned}
& (\nabla \cdot \mathbf{v}, \epsilon) \\
= & (\nabla \cdot (\mathbf{v} - \mathbf{v}_I), \epsilon) + (\nabla \cdot \mathbf{v}_I, \epsilon) \\
= & (\nabla \cdot (\mathbf{v} - \mathbf{v}_I), \epsilon) + (\nabla \mathbf{e}, \nabla \mathbf{v}_I) + \gamma \sum_{T \in \mathcal{T}_h} h_T^2 (\nabla \epsilon - \Delta \mathbf{e}, -\Delta \mathbf{v}_I)_T \\
= & (\nabla \cdot (\mathbf{v} - \mathbf{v}_I), \epsilon) - (\nabla \mathbf{e}, \nabla (\mathbf{v} - \mathbf{v}_I)) + (\nabla \mathbf{e}, \nabla \mathbf{v}) \\
& + \gamma \sum_{T \in \mathcal{T}_h} h_T^2 (\mathbf{f} + \Delta \mathbf{u}_h - \nabla p_h, -\Delta \mathbf{v}_I)_T \\
= & - \sum_{T \in \mathcal{T}_h} (\mathbf{f} + \Delta \mathbf{u}_h - \nabla p_h, \mathbf{v} - \mathbf{v}_I)_T + \sum_{T \in \mathcal{T}_h} \int_{\partial T} (\nabla \mathbf{u}_h - p_h \mathbf{I}) \cdot \mathbf{n} (\mathbf{v} - \mathbf{v}_I) ds \\
& + \gamma \sum_{T \in \mathcal{T}_h} h_T^2 (\mathbf{f} + \Delta \mathbf{u}_h - \nabla p_h, -\Delta \mathbf{v}_I)_T + (\nabla \mathbf{e}, \nabla \mathbf{v})_{\mathcal{T}_h} \\
\leq & C |\mathbf{v}|_1 \left( \left( \sum_{T \in \mathcal{T}_h} h_T^2 \|\mathbf{f} + \Delta \mathbf{u}_h - \nabla p_h\|_T^2 \right)^{1/2} \right. \\
& \left. + \left( \sum_{e \in \mathcal{E}_h^0} h_e \|\llbracket \nabla \mathbf{u}_h - p_h \mathbf{I} \rrbracket\|_e^2 \right)^{1/2} + \|\nabla \mathbf{e}\| \right).
\end{aligned}$$

Next, it follows from the inf-sup condition that

$$(10) \quad \|p - p_h\| \leq C \sup_{\mathbf{v} \in H_0^1(\Omega)^2} \frac{(\nabla \cdot \mathbf{v}, p - p_h)}{|\mathbf{v}|_1}.$$

Thus, we come up with the following estimate

$$\|p - p_h\| \leq C(\eta + \|\nabla \mathbf{e}\|).$$

This completes the proof of the lemma.  $\square$

**Theorem 2.** *Let  $(\mathbf{u}; p)$  and  $(\mathbf{u}_h; p_h)$  be the solutions of (1)-(2) and (4). Then we have the following global reliability bounds:*

$$(11) \quad \|\nabla(\mathbf{u} - \mathbf{u}_h)\| \leq C\eta$$

and

$$(12) \quad \|p - p_h\| \leq C\eta.$$

*Proof.* Let  $\mathbf{e}_I \in V_h$  be either the nodal value interpolation or the Clement interpolation of  $\mathbf{e}$ . Using integration by parts, equations (6), (8), the inverse inequality

and Lemma 1, we have

$$\begin{aligned}
& (\nabla \mathbf{e}, \nabla \mathbf{e}) = (\nabla \mathbf{e}, \nabla \mathbf{e} - \nabla \mathbf{e}_I) + (\nabla \mathbf{e}, \nabla \mathbf{e}_I) \\
= & (\nabla \mathbf{e}, \nabla \mathbf{e} - \nabla \mathbf{e}_I) + (\nabla \cdot \mathbf{e}_I, \epsilon) - \gamma \sum_{T \in \mathcal{T}_h} h_T^2 (\nabla \epsilon - \Delta \mathbf{e}, -\Delta \mathbf{e}_I)_T \\
= & (\nabla \mathbf{e}, \nabla \mathbf{e} - \nabla \mathbf{e}_I) - (\nabla \cdot (\mathbf{e} - \mathbf{e}_I), \epsilon) + (\nabla \cdot \mathbf{e}, \epsilon) \\
& - \gamma \sum_{T \in \mathcal{T}_h} h_T^2 (\mathbf{f} + \Delta \mathbf{u}_h - \nabla p_h, -\Delta \mathbf{e}_I)_T \\
= & \sum_{T \in \mathcal{T}_h} (\mathbf{f} + \Delta \mathbf{u}_h - \nabla p_h, \mathbf{e} - \mathbf{e}_I)_T - \sum_{T \in \mathcal{T}_h} \int_{\partial T} (\nabla \mathbf{u}_h - p_h \mathbf{I}) \cdot \mathbf{n} (\mathbf{e} - \mathbf{e}_I) ds \\
& - (\nabla \cdot \mathbf{u}_h, \epsilon) - \gamma \sum_{T \in \mathcal{T}_h} h_T^2 (\nabla \epsilon - \Delta \mathbf{e}, -\Delta \mathbf{e}_I)_T \\
\leq & C |\mathbf{e}|_1 \left( \left( \sum_{T \in \mathcal{T}_h} h_T^2 \|\mathbf{f} + \Delta \mathbf{u}_h - \nabla p_h\|_T^2 \right)^{1/2} + \left( \sum_{e \in \partial T} h_e \|\llbracket \nabla \mathbf{u}_h - p_h \mathbf{I} \rrbracket_e\|_e^2 \right)^{1/2} \right. \\
& \left. + \|\nabla \cdot \mathbf{u}_h\| (\eta + \|\nabla \mathbf{e}\|) \right) \\
\leq & C \eta^2 + \frac{1}{2} \|\nabla \mathbf{e}\|^2.
\end{aligned}$$

It follows that (11) holds true. The estimate (12) is a combined result of (11) and (9) of Lemma 1. This completes the proof.  $\square$

**3.2. Efficiency of the estimator.** For each triangle  $T \in \mathcal{T}_h$ , denote by  $\phi_T$  the following bubble function

$$\phi_T = \begin{cases} 27 \lambda_1 \lambda_2 \lambda_3 & \text{in } T, \\ 0 & \text{in } \Omega \setminus T, \end{cases}$$

where  $\lambda_i$ ,  $i = 1, 2, 3$  are barycentric coordinates on  $T$ . Needless to say, the finite element partition  $\mathcal{T}_h$  is assumed to contain triangular elements only in this part of the analysis. But we would like to point out that the analysis can be extended to quadrilateral elements without any difficulty. It is not hard to see that  $\phi_T \in H_0^1(\Omega)$  and satisfies the following properties [21]:

- For any polynomial  $q$  with degree at most  $m$ , there exist positive constants  $c_m$  and  $C_m$ , depending only on  $m$ , such that

$$(13) \quad c_m \|q\|_T^2 \leq \int_T q^2 \phi_T dx \leq \|q\|_T^2,$$

$$(14) \quad \|\nabla(q\phi_T)\|_T \leq C_m h_T^{-1} \|q\|_T.$$

For each  $e \in \mathcal{E}_h^0$ , we can analogously define an edge bubble function  $\phi_e$ . Let  $T_1$  and  $T_2$  be two triangles sharing the edge  $e$ . To this end, denote by  $\omega_e = T_1 \cup T_2$  the union of the elements  $T_1$  and  $T_2$ . Assume that in  $T_i$ ,  $i = 1, 2$ , the barycentric coordinates associated with the two ends of  $e$  are  $\lambda_1^{T_i}$  and  $\lambda_2^{T_i}$ , respectively. The edge bubble function can be defined as follows

$$\phi_e = \begin{cases} 4\lambda_1^{T_1} \lambda_2^{T_1} & \text{in } T_1, \\ 4\lambda_1^{T_2} \lambda_2^{T_2} & \text{in } T_2, \\ 0 & \text{in } \Omega \setminus \omega_e. \end{cases}$$

It is obvious that  $\phi_e \in H_0^1(\Omega)$  and satisfies the following properties [21]:

- For any polynomial  $q$  with degree at most  $m$ , there exist positive constants  $d_m$ ,  $D_m$  and  $E_m$ , depending only on  $m$ , such that

$$(15) \quad d_m \|q\|_e^2 \leq \int_e q^2 \phi_e ds \leq \|q\|_e^2,$$

$$(16) \quad \|\nabla(q\phi_e)\|_{\omega_e} \leq D_m h_e^{-1/2} \|q\|_e,$$

$$(17) \quad \|q\phi_e\|_{\omega_e} \leq E_m h_e^{1/2} \|q\|_e.$$

For every  $T \in \mathcal{T}_h$ , let  $\mathbf{f}_T$  be the mean value of  $\mathbf{f}$  on  $T$ . We have the following efficiency bounds.

**Theorem 3.** *Under the same assumption as Theorem 2, there exists a generic constant  $C > 0$  such that*

$$(18) \quad \|\mathbf{f}_T + \Delta \mathbf{u}_h - \nabla p_h\|_T \leq C(\|\nabla(\mathbf{u} - \mathbf{u}_h)\|_T + \|p - p_h\|_T + h\|\mathbf{f} - \mathbf{f}_T\|_T),$$

$$(19) \quad h^{1/2} \|\llbracket \nabla \mathbf{u}_h - p_h I \rrbracket\|_e \leq C(h\|\mathbf{f} - \mathbf{f}_T\|_{\omega_e} + \|\nabla(\mathbf{u} - \mathbf{u}_h)\|_{\omega_e} + \|p - p_h\|_{\omega_e}),$$

$$(20) \quad \|\nabla \cdot \mathbf{u}_h\|_T \leq C\|\nabla \mathbf{e}\|_T.$$

Consequently, there is a constant  $C$  such that

$$(21) \quad \eta^2 \leq C \left( \|\nabla(\mathbf{u} - \mathbf{u}_h)\|^2 + \|p - p_h\|^2 + \sum_T h_T^2 \|\mathbf{f} - \mathbf{f}_T\|_T^2 \right).$$

*Proof.* Let  $\mathbf{w}_T = (\mathbf{f}_T + \Delta \mathbf{u}_h - \nabla p_h)\phi_T(x)$ . Then we have

$$(\mathbf{f}, \mathbf{w}_T)_T = (\nabla \mathbf{u}, \nabla \mathbf{w}_T)_T - (\nabla \cdot \mathbf{w}_T, p)_T.$$

Adding and subtracting  $(\mathbf{f}_T, \mathbf{w}_T)_T$ ,  $(\nabla \mathbf{u}_h, \nabla \mathbf{w}_T)_T$  and  $(\nabla \cdot \mathbf{w}_T, p_h)_T$  to the above equation and using integration by parts yields the following

$$(\mathbf{f} - \mathbf{f}_T, \mathbf{w}_T)_T + (\mathbf{f}_T + \Delta \mathbf{u}_h - \nabla p_h, \mathbf{w}_T)_T = (\nabla \mathbf{e}, \nabla \mathbf{w}_T)_T - (\nabla \cdot \mathbf{w}_T, \epsilon)_T.$$

The properties of the bubble function  $\phi_T(x)$  implies

$$\begin{aligned} \|\mathbf{f}_T + \Delta \mathbf{u}_h - \nabla p_h\|_T^2 &\leq C \left( h^{-1} (\|\nabla \mathbf{e}\|_T + \|\epsilon\|_T) \|\mathbf{f}_T + \Delta \mathbf{u}_h - \nabla p_h\|_T \right. \\ &\quad \left. + \|\mathbf{f} - \mathbf{f}_T\|_T \|\mathbf{f}_T + \Delta \mathbf{u}_h - \nabla p_h\|_T \right). \end{aligned}$$

Thus, it follows from the above estimate and the triangle inequality that

$$(22) \quad h\|\mathbf{f}_T + \Delta \mathbf{u}_h - \nabla p_h\|_T \leq C(\|\nabla \mathbf{e}\|_T + \|\epsilon\|_T + h\|\mathbf{f} - \mathbf{f}_T\|_T),$$

which verifies the inequality (18).

To establish (19), we set  $\mathbf{w}_e = \llbracket \nabla \mathbf{u}_h - p_h I \rrbracket \phi_e(x)$ . Using integration by parts, we have

$$(23) \quad \begin{aligned} (\nabla \mathbf{u}_h, \nabla \mathbf{w}_e)_{\omega_e} &= - \sum_{T \in \omega_e} (\Delta \mathbf{u}_h, \mathbf{w}_e)_T + \sum_{T \in \omega_e} (\nabla \mathbf{u}_h \cdot \mathbf{n}, \mathbf{w}_e)_{\partial T} \\ &= - \sum_{T \in \omega_e} (\Delta \mathbf{u}_h, \mathbf{w}_e)_T + \int_e \llbracket \nabla \mathbf{u}_h \rrbracket \cdot \mathbf{w}_e ds, \end{aligned}$$

and

$$\begin{aligned}
(\nabla \cdot \mathbf{w}_e, p_h)_{\omega_e} &= - \sum_{T \in \omega_e} (\nabla p_h, \mathbf{w}_e)_T + \sum_{T \in \omega_e} (p_h \mathbf{n}, \mathbf{w}_e)_{\partial T} \\
(24) \qquad \qquad \qquad &= - \sum_{T \in \omega_e} (\nabla p_h, \mathbf{w}_e)_T + \int_e [[p_h I]] \cdot \mathbf{w}_e ds.
\end{aligned}$$

Testing (1) by  $\mathbf{w}_e$  over  $\omega_e$  and using integration by parts gives

$$(25) \qquad \qquad \qquad (\mathbf{f}, \mathbf{w}_e)_{\omega_e} = (\nabla \mathbf{u}, \nabla \mathbf{w}_e)_{\omega_e} - (\nabla \cdot \mathbf{w}_e, p)_{\omega_e}.$$

Subtracting (24) from (23), using the property of the bubble function  $\phi_e(x)$  and the identity (25), we arrive at

$$\begin{aligned}
& \|[\nabla \mathbf{u}_h - p_h I]\|_e^2 \\
& \leq C \sum_{T \in \omega_e} \left( (\Delta \mathbf{u}_h - \nabla p_h, \mathbf{w}_e)_T + (\nabla \mathbf{u}_h, \nabla \mathbf{w}_e)_T - (\nabla \cdot \mathbf{w}_e, p_h)_T \right) \\
& \leq C \sum_{T \in \omega_e} \left( (\mathbf{f} - \mathbf{f}_T, \mathbf{w}_e)_T + (\mathbf{f}_T + \Delta \mathbf{u}_h - \nabla p_h, \mathbf{w}_e)_T \right. \\
& \qquad \qquad \qquad \left. - (\nabla \mathbf{e}, \nabla \mathbf{w}_e)_T + (\epsilon, \nabla \cdot \mathbf{w}_e)_T \right) \\
& \leq C \|[\nabla \mathbf{u}_h - p_h I]\|_e \left( h^{1/2} \|\mathbf{f} - \mathbf{f}_T\|_{\omega_e} + h^{1/2} \|\mathbf{f}_T + \Delta \mathbf{u}_h - \nabla p_h\|_{\omega_e} \right. \\
& \qquad \qquad \qquad \left. + h^{-1/2} \|\nabla \mathbf{e}\|_{\omega_e} + h^{-1/2} \|\epsilon\|_{\omega_e} \right).
\end{aligned}$$

Consequently,

$$(26) \qquad h^{1/2} \|[\nabla \mathbf{u}_h - p_h I]\|_e \leq C (h \|\mathbf{f} - \mathbf{f}_T\|_{\omega_e} + \|\nabla \mathbf{e}\|_{\omega_e} + \|\epsilon\|_{\omega_e}).$$

Finally, we define  $q_T = \nabla \cdot \mathbf{u}_h \phi_T(x)$  and test (2) by  $q_T$  over  $T \in \mathcal{T}_h$  to obtain

$$(\nabla \cdot \mathbf{u}, q_T)_T = 0.$$

Therefore,

$$(\nabla \cdot \mathbf{u}_h, q_T)_T = (\nabla \cdot (\mathbf{u}_h - \mathbf{u}), q_T)_T.$$

Using the properties of the bubble function  $\phi_T(x)$ , we have

$$\|\nabla \cdot \mathbf{u}_h\|_T \leq C \|\nabla \mathbf{e}\|_T.$$

This completes the proof of (20).  $\square$

#### 4. Numerical results

This section shall report some computational results for the error estimator when a nonsymmetric formulation is used with the stabilized  $P_2/P_1$  element. The resulting linear system from this discretization is solved by using the BiConjugate Gradient (BICG) method with a relative residual of  $10^{-8}$  as the stopping criteria.

**4.1. Test problems.** Three test problems are considered in this numerical investigation; all are defined on the unit square domain  $\Omega = (0, 1) \times (0, 1)$ . Two of them have exact solutions given as:

$$\begin{aligned}
\text{Test problem 1:} \quad \mathbf{u} &= \begin{pmatrix} -2x^2y(x-1)^2(2y-1)(y-1) \\ xy^2(2x-1)(x-1)(y-1)^2 \end{pmatrix}, \\
p &= \sin(\pi x) \sin(\pi y) - \frac{4}{\pi^2},
\end{aligned}$$



and

$$\textbf{Test problem 2: } \quad \mathbf{u} = \begin{pmatrix} \frac{3}{2}\sqrt{r}(\cos\frac{\theta}{2} - \cos\frac{3\theta}{2}) \\ \frac{3}{2}\sqrt{r}(3\sin\frac{\theta}{2} - \sin\frac{3\theta}{2}) \end{pmatrix}, \quad p = -6r^{-1/2}\cos\frac{\theta}{2}.$$

Observe that the test problem 2 has a corner singularity of order 0.5 at the origin  $(0,0)$ . The third problem is the 2D lid driven cavity problem, which describes the flow in a rectangular container driven by the uniform motion of the top lid [19]. Due to the discontinuity of the velocity boundary condition at two top corners, the exact solution  $(\mathbf{u}; p)$  of the Stokes equation does not belong to  $(H^1)^2 \times L^2$ , if there is any in the sense of distribution. Indeed, the usual weak formulation does not make sense for this problem because of the said singularity. However, the discrete problem is still well-posed and provides a certain approximation to the actual solution. In two dimensional case, the discontinuous boundary condition also results in corner singularities at the two top corners.

**4.2. On uniform meshes.** In this experiment, we solve test problems 1 and 2 on uniform meshes and analyze the asymptotic order of the error estimator  $\eta$ . The coarsest mesh is generated by dividing  $\Omega$  into  $4 \times 4$  sub-rectangles, and then dividing each sub-rectangle into four triangles by connecting its two diagonal lines. We then apply the usual uniform refinement procedure, which divides each triangle into four sub-triangles by connecting the center of its three edges, to get several levels of fine meshes.

For test problem 1, we know that in theory  $\eta = O(h^2)$ . For test problem 2, the order of  $\eta$  is expected to be  $O(h^{0.5})$ . Numerical results for these two test problems are reported in tables 1 and 2. In these tables,  $\|\mathbf{u} - \mathbf{u}_h\|_\infty$  is defined as the maximum norm error measured on all  $P_2$  nodes, that is, all vertices of  $\mathcal{T}_h$  and the center of all edges in  $\mathcal{E}_h$ . Similarly,  $\|p - p_h\|_\infty$  is the maximum norm error measured for the pressure on all nonconforming  $P_1$  nodes, that is, vertices of all triangles in  $\mathcal{T}_h$ . For test problem 2, the error for the pressure approximation is not calculated since the pressure goes to infinity at the singular point  $(0,0)$ .

From Table 1, it seems that the value of  $\beta$  does not affect the asymptotic order for  $\eta$ , while  $\gamma$  needs to be small. The theoretical results stated that  $\gamma$  and  $\beta$  can be arbitrary positive numbers, for the nonsymmetric formulation was employed in the numerical discretization. However, we suspect that a larger value of  $\gamma$  may cause the linear system to be unexpectedly ill-conditioned, for which the iterative solver may have trouble to handle without using a good preconditioner. This might explain the deterioration of convergence rates observed for large  $\gamma$ . The numerical results with  $\gamma = 0.01$  and  $\beta = 1$  are in good agreement with theoretical predictions. This motivated the use of  $\gamma = 0.01$  and  $\beta = 1$  in our numerical experiments for test problem 2 as illustrated in Table 2.

**4.3. Adaptive local refinements.** We also tested some adaptive local refinement strategies for test problems 2 and 3, which have corner singularities. Two different refinement strategies are considered in this study. The first one is based on a comparison of each error  $\eta_T$  with the maximum value of all the error estimators. The strategy can be described as follows:

**Local Refinement by ‘‘Maximum Strategy’’:**

- (1) Given a current triangular mesh, error indicators  $\eta_T$  on each triangle, and a threshold  $\theta \in (0,1)$  (eg.,  $\theta = 0.5$ ). One computes the maximum error  $\eta_{max} = \max \eta_T$ .
- (2) For each triangle  $T$ , if  $\eta_T \geq \theta \eta_{max}$ , mark this triangle for refinement.

TABLE 1. Convergence behavior for test problem 1 on  $n \times n$  uniform triangular meshes.

	$h$	$\eta$	$\ \nabla(\mathbf{u} - \mathbf{u}_h)\ $	$\ \mathbf{u} - \mathbf{u}_h\ _\infty$	$\ p - p_h\ $	$\ p - p_h\ _\infty$
$\gamma = 0$ $\beta = 0$	1/4	5.17e-02	8.74e-03	3.31e-04	1.21e-02	6.21e-02
	1/8	4.16e-02	2.57e-03	7.64e-05	7.36e-03	5.73e-02
	1/16	3.27e-02	8.96e-04	2.50e-05	5.91e-03	5.02e-02
	1/32	2.67e-02	3.73e-04	8.93e-06	4.82e-03	3.29e-02
	$k$ in $O(h^k)$	0.3213	1.5175	1.7257	0.4322	0.2940
$\gamma = 1$ $\beta = 100$	1/4	3.34e-02	1.47e-02	1.24e-03	1.43e-02	7.44e-02
	1/8	1.22e-02	5.00e-03	1.91e-04	3.62e-03	2.10e-02
	1/16	3.07e-03	1.18e-03	2.81e-05	7.80e-04	5.45e-03
	1/32	7.26e-04	2.45e-04	3.72e-06	1.83e-04	1.37e-03
	$k$ in $O(h^k)$	1.8564	1.9797	2.7938	2.1072	1.9229
$\gamma = 1$ $\beta = 10^{-6}$	1/4	3.21e-02	1.05e-02	4.24e-04	1.29e-02	7.53e-02
	1/8	1.28e-02	2.37e-03	4.91e-05	2.93e-03	1.92e-02
	1/16	3.42e-03	5.69e-04	8.32e-06	7.14e-04	5.20e-03
	1/32	1.19e-03	3.40e-04	1.48e-05	3.98e-04	7.36e-03
	$k$ in $O(h^k)$	1.6148	1.6906	1.7081	1.7101	1.1951
$\gamma = 0.01$ $\beta = 1$	1/4	2.71e-02	9.81e-03	4.80e-04	1.12e-02	6.29e-02
	1/8	9.01e-03	2.39e-03	5.54e-05	2.86e-03	1.47e-02
	1/16	2.42e-03	5.73e-04	5.66e-06	7.15e-04	3.67e-03
	1/32	6.25e-04	1.39e-04	7.26e-07	1.78e-04	9.16e-04
	$k$ in $O(h^k)$	1.8211	2.0466	3.1398	1.9932	2.0310

TABLE 2. Convergence behavior for test problem 2 on  $n \times n$  uniform triangular meshes, with  $\gamma = 0.01$  and  $\beta = 1$ .

$h$	dofs	$\eta$	$\ \nabla(\mathbf{u} - \mathbf{u}_h)\ $	$\ \mathbf{u} - \mathbf{u}_h\ _\infty$
1/4	482	2.2560	0.8599	0.0897
1/8	1858	1.4783	0.6066	0.0695
1/16	7298	1.0208	0.4281	0.0492
1/32	28930	0.7223	0.3027	0.0348
Asym. Order $O(h^k)$ , $k =$	-1.9696	0.5463	0.5021	0.4594

- (3) The actual refinement is done by the newest node bisection method as explained in [16, 18]. It has been proved that this method will not cause mesh degeneration. The only requirement is that the “newest nodes” for the coarsest mesh must be assigned carefully such that every triangle is compatibly divisible. This can be easily checked.

The second refinement strategy is based on a comparison of  $\eta_T$  with those for its neighbors. To explain the main idea, let  $\rho > 0$  be a prescribed distance parameter

TABLE 3. Convergence behavior for test problem 2 using adaptive mesh refinements, with  $\gamma = 0.01$  and  $\beta = 1$ .

Strategy	Refinement times	dofs	$\eta$	$\ \nabla(\mathbf{u} - \mathbf{u}_h)\ $	$\ \mathbf{u} - \mathbf{u}_h\ _\infty$
Maximum	0	482	2.2560	0.8599	0.0897
	8	638	0.8705	0.3240	0.0225
	16	1143	0.3494	0.1238	0.0054
Local	0	482	2.2560	0.8599	0.0897
	8	782	0.7309	0.2672	0.0224
	16	1497	0.2502	0.1028	0.0065

FIGURE 1. Test problem 2, maximum strategy adaptive refinement, with  $\gamma = 0.01$  and  $\beta = 1$ . Meshes after 0, 8, and 16 refinements.

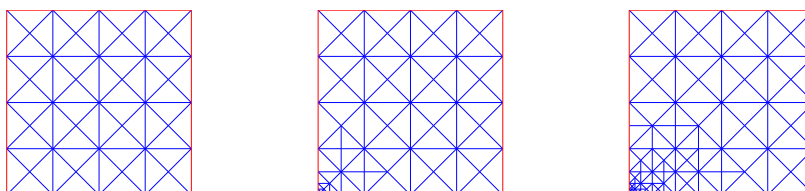
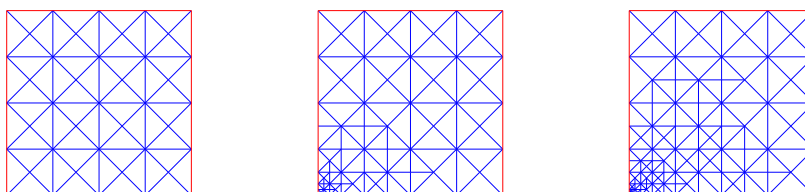


FIGURE 2. Test problem 2, local strategy adaptive refinement, with  $\gamma = 0.01$  and  $\beta = 1$ . Meshes after 0, 8, and 16 refinements.



and set

$$\mathcal{T}_{\rho,T} = \{\tilde{T} : 0 < \|T - \tilde{T}\| \leq \rho\},$$

where  $\|T - \tilde{T}\|$  stands for the distance of the centers of  $T$  and  $\tilde{T}$ . With a given threshold  $\theta > 1$ , we mark a triangle  $T$  for refinement if

$$\eta_T \geq \theta \eta_{N(T)},$$

where  $\eta_{N(T)}$  is the average of the local error indicator on all the neighboring triangles  $\tilde{T} \in \mathcal{T}_{\rho,T}$ .

The following is such a refinement strategy that was numerically investigated in this study.

**Local Refinement by “Local Strategy”:**

- (1) Given a current triangular mesh, error estimators  $\eta_T$  on each triangle, and a threshold  $\theta > 1.0$  (e.g.,  $\theta = 1.5$ ). One computes an error indicator  $\eta_{N(T)}$

FIGURE 3. Test problem 2, maximum strategy adaptive refinement, with  $\gamma = 0.01$  and  $\beta = 1$ . Plot of  $\eta$ ,  $\|\nabla(\mathbf{u} - \mathbf{u}_h)\|$  and  $\|\mathbf{u} - \mathbf{u}_h\|_\infty$ , versus the degrees of freedom  $N$ .

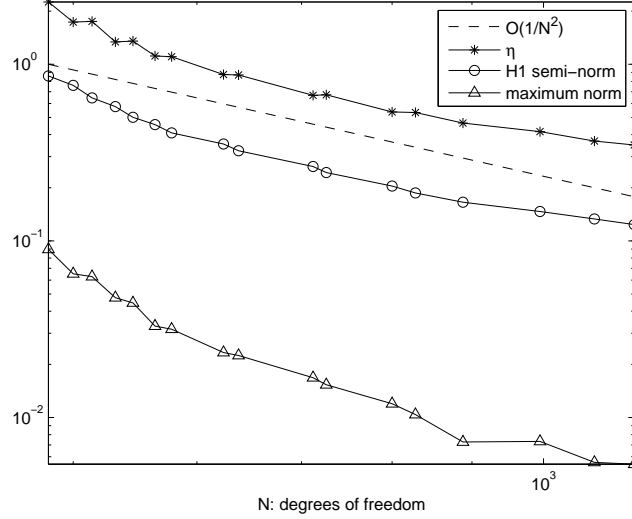
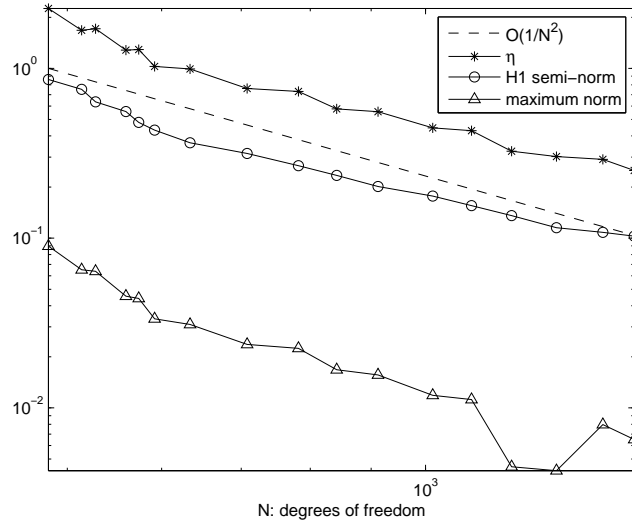


FIGURE 4. Test problem 2, local strategy adaptive refinement, with  $\gamma = 0.01$  and  $\beta = 1$ . Plot of  $\eta$ ,  $\|\nabla(\mathbf{u} - \mathbf{u}_h)\|$  and  $\|\mathbf{u} - \mathbf{u}_h\|_\infty$ , versus the degrees of freedom  $N$ .



as the average of the local error indicator on neighboring triangles that share a vertex or an edge with  $T$ , not including  $T$  itself.

- (2) For each triangle  $T$ , if  $\eta_T \geq \theta \eta_{N(T)}$ , mark this triangle for refinement.

- (3) The actual refinement is again done by the newest node bisection method [16, 18].

We first examine the case with  $\gamma = 0.01$  and  $\beta = 1$ . The residual estimator and errors for test problem 2, using adaptive mesh refinements, are reported in Table 3. By comparing tables 2 and 3, one clearly sees the advantage of using adaptive refinements. The corresponding meshes after 0, 8, and 16 refinements are drawn in figures 1 and 2, which indicate that our residual estimator captures the corner singularity correctly, under both refinement strategies. Furthermore, in figures 3 and 4, we examine the relation of  $\eta$ ,  $\|\nabla(\mathbf{u} - \mathbf{u}_h)\|$  and  $\|\mathbf{u} - \mathbf{u}_h\|_\infty$  with the degrees of freedom  $N$  during the process of the adaptive refinement. The plots start from the coarsest mesh and ends after 16 refinements.

For  $\gamma = 1$  and  $\beta = 100$ , similar results have been observed for test problem 2. As was conjectured earlier, the system becomes extremely ill-conditioned in the refining process, and the error gets large after certain steps. However, the error indicator still locates the corner singularity correctly. These results are reported in Table 4, Figures 5, 6, 7, and 8.

Finally, we report the results of the adaptive refinements for the driven cavity problem. Since the exact solution is not even in  $(H^1)^2 \times L^2$ , we expect that  $\eta$  does not decrease when the mesh is refined. Our experiments show that the error indicator  $\eta_T$  is able to locate both corner singularities for this problem. For  $\gamma = 0.01$  and  $\beta = 1$ , the meshes after 0, 8, and 16 refinements are plotted in figures 9 and 10.

TABLE 4. Convergence behavior for test problem 2 using adaptive mesh refinements, with  $\alpha = 1$  and  $\beta = 100$ .

Strategy	Refinement times	dofs	$\eta$	$\ \nabla(\mathbf{u} - \mathbf{u}_h)\ $	$\ \mathbf{u} - \mathbf{u}_h\ _\infty$
Maximum	0	482	2.2560	0.8599	0.0897
	8	806	0.6587	0.2749	0.0224
	16	1140	0.2797	0.1161	0.0109
Local	0	482	2.2560	0.8599	0.0897
	8	760	0.7676	0.3381	0.0316
	16	1089	0.4403	0.1979	0.0206

FIGURE 5. Test problem 2, maximum strategy adaptive refinement, with  $\alpha = 1$  and  $\beta = 100$ . Meshes after 0, 8, and 16 refinements.

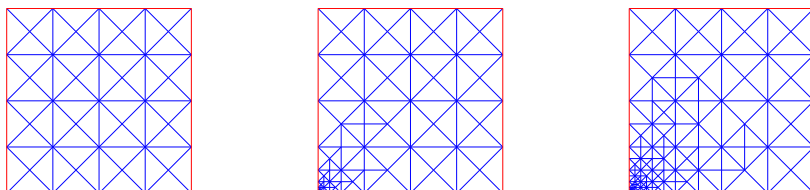


FIGURE 6. Test problem 2, local strategy adaptive refinement, with  $\alpha = 1$  and  $\beta = 100$ . Meshes after 0, 8, and 16 refinements.

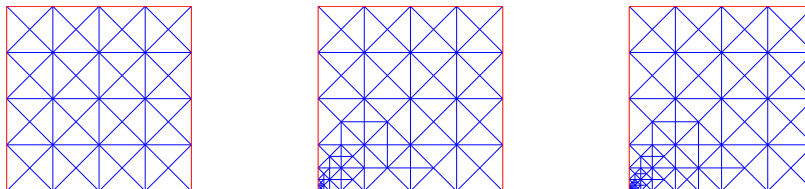
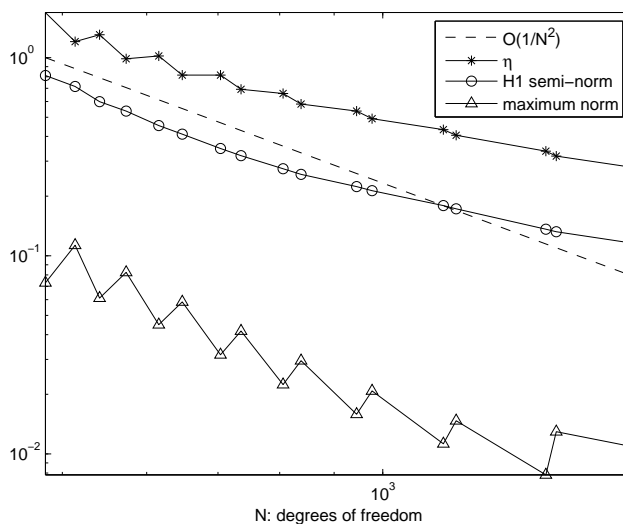


FIGURE 7. Test problem 2, maximum strategy adaptive refinement, with  $\alpha = 1$  and  $\beta = 100$ . Plot of  $\eta$ ,  $\|\nabla(\mathbf{u} - \mathbf{u}_h)\|$  and  $\|\mathbf{u} - \mathbf{u}_h\|_\infty$ , versus the degrees of freedom  $N$ .



## References

- [1] I. BABUŠKA, *The finite element method with Lagrangian multiplier*, Numer. Math., 20 (1973), 179-192.
- [2] B. BREFORT, *Attractor for the penalty Navier-Stokes equations*, SIAM J. Math. Anal., 19 (1988), 1-21.
- [3] F. BREZZI, *On the existence, uniqueness, and approximation of saddle point problems arising from Lagrangian multipliers*, R.A.I.R.O., Anal. Numér., 2 (1974), 129-151.
- [4] F. BREZZI AND J. DOUGLAS, *Stabilized mixed methods for the Stokes problem*, Numer. Math., 53 (1988), 225-235.
- [5] P. BOCHEV AND M. GUNZBURGER, *An absolutely stable pressure-poisson stabilized finite element method for the Stokes equations*, SIAM J. Numer. Anal., 42 (2004), 1189-1207.
- [6] P. G. CIARLET, *The Finite Element Method for Elliptic Problems*, North-Holland, New York, 1978.
- [7] M. CROUZEIX AND P. A. RAVIART, *Conforming and non-conforming finite element methods for solving the stationary Stokes equations*, R.A.I.R.O. R3 (1973), 33-76.
- [8] J. DOUGLAS AND J. WANG, *An absolutely stabilized finite element method for the Stokes problem*, Math. Comp., 52 (1989), 495-508.

FIGURE 8. Test problem 2, local strategy adaptive refinement, with  $\alpha = 1$  and  $\beta = 100$ . Plot of  $\eta$ ,  $\|\nabla(\mathbf{u} - \mathbf{u}_h)\|$  and  $\|\mathbf{u} - \mathbf{u}_h\|_\infty$ , versus the degrees of freedom  $N$ .

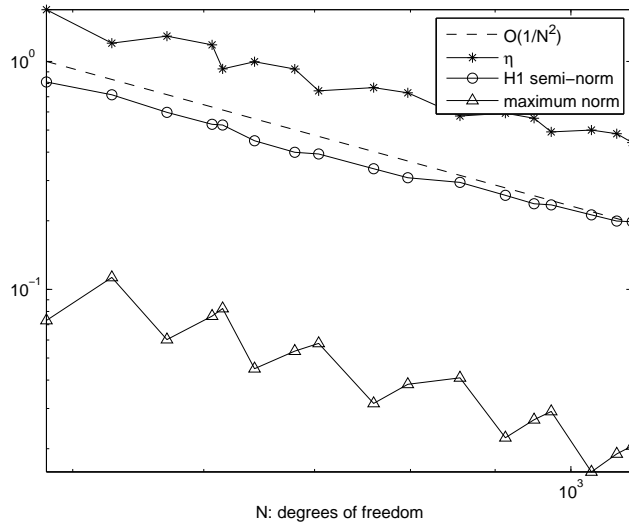


FIGURE 9. Test problem 3, maximum adaptive refinement, with  $\gamma = 0.01$  and  $\beta = 1$ . Meshes after 0, 8, and 16 refinements.

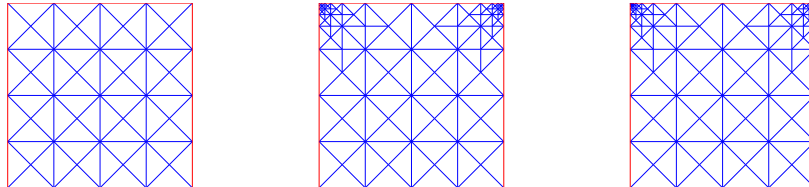
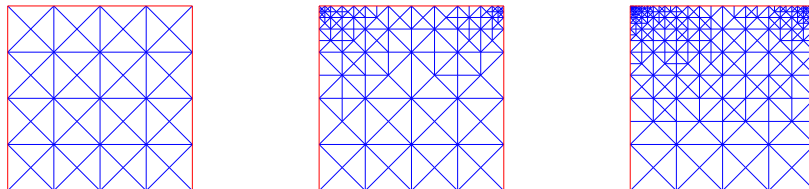


FIGURE 10. Test problem 3, local adaptive refinement, with  $\gamma = 0.01$  and  $\beta = 1$ . Meshes after 0, 8, and 16 refinements.



[9] V. GIRAULT AND P.A. RAVIART, *Finite Element Methods for the Navier-Stokes Equations: Theory and Algorithms*, Springer, Berlin, 1986.  
 [10] M. D. GUNZBURGER, *Finite Element Methods for Viscous Incompressible Flows, A Guide to Theory, Practice and Algorithms*, Academic Press, San Diego, 1989.

- [11] G.C. BUSCAGLIAA, F.G. BASOMBRIO AND R. CODINAB, *Fourier analysis of an equal-order incompressible flow solver stabilized by pressure gradient projection*, Int. J. Numer. Meth. Fluids 34(2000), 65-92.
- [12] T. HUGHES, L. FRANCA AND M. BALESTRA, *A new finite element formulation for computational fluid dynamics: V. Circumventing the Babuška-Brezzi condition: A stable Petrov-Galerkin formulation of the Stokes problem accommodating equal-order interpolation*, Comput. Meth. Appl. Mech. Engng., 59 (1986), 85-99.
- [13] T. HUGHES AND L. FRANCA, *A new finite element formulation for computational fluid dynamics: VII. The Stokes problem with various well-posed boundary conditions: symmetric formulations that converge for all velocity/pressure spaces*, Comput. Meth. Appl. Mech. Engng., 65 (1987) 85-96.
- [14] D. KAY AND D. SILVESTER *A posteriori error estimation for stabilised mixed approximations of the Stokes equations*, SIAM J. Scientific Computing 21, (1999), 1321-1336.
- [15] J. LI, J. WANG AND X. YE *Superconvergence by  $L^2$ -projections for stabilized finite element methods for the Stokes equations*, IJNAM, 6 (2009), 711-723.
- [16] W. F. MITCHELL *Unified Multilevel Adaptive Finite Element Methods for Elliptic Problems*, Ph.D. dissertation, University of Illinois at Urbana-Champaign, 1988.
- [17] W. HOPFMANN, A. H. SCHATZ, L. B. WAHLBIN, AND G. WITTUM, *Asymptotically exact a posteriori estimators for the pointwise gradient error on each element in irregular meshes. Part 1: A smooth problem and globally quasi-uniform meshes*, Math. Comp., 70 (2001), 897-909.
- [18] E. G. SEWELL, *Automatic generation of triangulations for piecewise polynomial approximation*, Ph.D. dissertation, Purdue University, 1972.
- [19] P.N. SHANKAR AND M.D. DESHPANDE, *Fluid Mechanics in the driven cavity*, Annu. Rev. Fluid Mech., 32 (2000), pp. 93-136.
- [20] J. SHEN, *On error estimates of the penalty method for unsteady Navier-Stokes equations*, SIAM J. Numer. Anal., 32 (1995), 386-403.
- [21] R. VERFURTH, *A review of a posteriori error estimation and adaptive mesh-refinement techniques*. Teubner Skripten zur Numerik. B.G. Willey-Teubner, Stuttgart, 1996.

Division of Mathematical Sciences, National Science Foundation, Arlington, VA 22230, USA  
*E-mail:* [jwang@nsf.gov](mailto:jwang@nsf.gov)

Department of Mathematics, Oklahoma State University, Stillwater, OK 74075, USA  
*E-mail:* [yqwang@math.okstate.edu](mailto:yqwang@math.okstate.edu)

Department of Mathematics, University of Arkansas at Little Rock, Little Rock, AR 72204, USA  
*E-mail:* [xxye@ualr.edu](mailto:xxye@ualr.edu)